DEUTSCHES ELEKTRONEN-SYNCHROTRON DESY

DESY 83-085
September 1983

LATEST RESULTS ON HADRON PRODUCTION AT PETRA

by

H. Rykaczewski

National Institute for Nuclear and High Energy Physics NIKHEF, Amsterdam

ISSN 0418-9833

NOTKESTRASSE 85 · 2 HAMBURG 52

To be sure that your preprints are promptly included in the
HIGH ENERGY PHYSICS INDEX ,
send them to the following address (if possible by air mail) :

DESY
Bibliothek
Notkestrasse 85
2 Hamburg 52
Germany

DESY 83-085
September 1983

ISSN 0418-9833

LATEST RESULTS ON HADRON PRODUCTION AT PETRA

Hans Rykaczewski

National Institute for Nuclear and
High Energy Physics NIKHEF
Amsterdam, The Netherlands

ABSTRACT

Some of the prime objectives of investigations of hadron production via $e^+ e^-$ annihilation are the searches for new quark flavors and studies of electroweak effects due to the interference of virtual γ - and Z^0 - exchange. By measuring the total hadronic cross-section R and the structure of hadronic events, we exclude the continuum production of top quarks up to c.m. energies of more than 40 GeV. Using the R-measurements we determine $\sin^2\vartheta_w$ at high Q^2.

Analyses of hadronic final states produced by two-photon interactions lead to results on meson resonance production and the photon structure function F_2.

Invited talk at the Asia Pacific Physics Conference, Singapore, 12-18 June 1983

1. INTRODUCTION

In this talk I will review hadron production in $e^+ e^-$ interactions at PETRA, the electron - positron colliding beam storage ring at DESY in Hamburg, Germany. Since the end of 1978 the five experiments CELLO, JADE, MARK-J, PLUTO and TASSO have been taking data at c.m. energies between $\sqrt{s}$ = 12 GeV and $\sqrt{s}$ = 43 GeV. By mid 1983 up to 37000 multihadron events per experiment were detected, corresponding to an integrated luminosity of approximately 100 pb^{-1}.

Measurements of hadron production via one photon annihilation, which will be discussed in Chapter 2, enable the experiments to search for the production of a new quark flavor, the so called top with a charge $\frac{2}{3}$ e. Measurements of the total cross-section R, the search for narrow quark-antiquark bound states and the analysis of the shape of multihadron events yield lower limits on the mass of such a new quark. The results of searches for flavor-changing neutral currents in bottom quark decays exclude models without the top quark. Since the hadronic cross-section is sensitive not only to the production of new quark flavors, but also to interference effects between the virtual γ and Z^0, these results measure the electroweak mixing angle $\sin^2\vartheta_w$ at high Q^2 including the effects of heavy quarks.

Analyses of hadronic final states produced by two photon interactions will be presented in Chapter 3. These events exhibit clear resonance signals and the latest results on the radiative widths for f and A_2 mesons will be given. Description of the deep inelastic electron photon process $e + \gamma \longrightarrow e +$ hadrons in terms of two photon interactions leads to results on the photon structure function F_2 and allows comparisons with QCD predictions.

2. ONE PHOTON ANNIHILATION

2.1. Total hadronic cross-section

In lowest order $e^+ e^-$ annihilate to a timelike photon which couples directly [1-4] to a quark-antiquark pair ($q\bar{q}$) as shown in Fig. 1. Both, the quark and the antiquark, begin to move apart and

fragment, i.e. they pull additional $q\bar{q}$ pairs from the vacuum thus forming two jets of hadrons along the direction of the primary quarks.

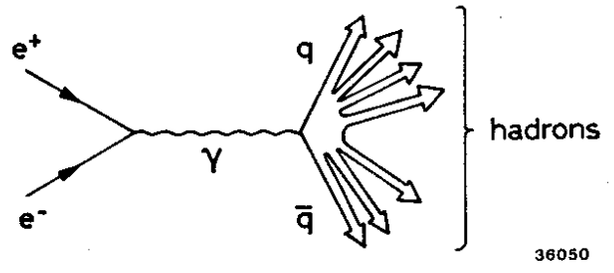

Figure 1: Feynman graph for hadron production via one photon annihilation.

The cross-section of this electromagnetic process is usually normalised to the pointlike QED cross-section, σ_{point}, and defined as :

$$R = \frac{\sigma(e^+e^- \longrightarrow \text{hadrons})}{\sigma_{point}} \qquad (1)$$

The pointlike QED cross-section is given by :

$$\sigma_{point} = \frac{4\,\pi\,\alpha^2}{3\,s} = 86.85\ \text{nb}\ \frac{\text{GeV}^2}{s} \qquad (2)$$

where α is the electromagnetic coupling constant, $\alpha = 1/137.04$, and s is the c.m. energy squared.

In the quark-parton model (QPM) R can be written as

$$R_{QPM} = 3 \cdot \sum_{i}^{N_f} Q_i^2 , \qquad (3)$$

where Q_i is the charge of the quark with flavor i. The sum is to taken over all produced quark flavors (up to N_f) and the factor 3 accounts for different colors.

In the framework of Quantum Chromodynamics (QCD) one must take gluon-bremsstrahlung and higher order effects [5-8] into account. These corrections modify the hadronic cross-section[9-11]. In the $\overline{MS}$ renormalisation scheme :

$$R_{QCD} = R_{QPM}\left(1 + \frac{\alpha_s}{\pi} + (1.98 - 0.115 \cdot N_f) \cdot \frac{\alpha_s^2}{\pi^2}\right), \qquad (4)$$

where α_s denotes the coupling constant of the strong interaction. Using complete second order [12] Monte Carlo calculations, α_s has recently been measured at PETRA to be $\alpha_s \approx 0.13 - 0.16$, and results in an energy dependent correction of about 4% to 6% of R_{QPM}.

Electroweak effects, where the timelike current can be carried either by a virtual photon (Fig. 1) or by a virtual Z^0 (Fig. 2), cause additional modification of the hadronic cross-section.

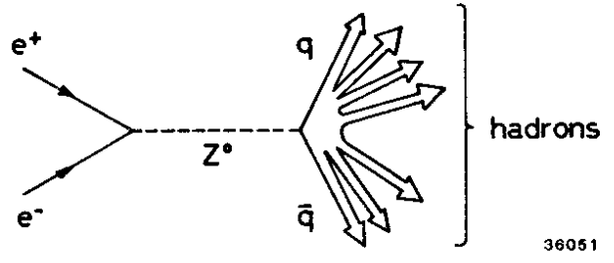

Figure 2: Feynman diagram of hadronic final state production by virtual Z^0 decay.

For a quark of flavor i the cross-section [13-14] is:

$$R^{i}_{QCD,EW}=[Q_i^2 - 8\cdot s\cdot g\cdot Q_i\cdot gv_e\cdot gv_q\cdot\eta + 16\cdot s^2\cdot g^2(gv_e^2+ga_e^2)(gv_q^2+ga_q^2)\eta^2]$$

$$\cdot [1 + \frac{\alpha_s}{\pi} + (1.98-0.115\cdot N_f)\cdot\frac{\alpha_s^2}{\pi^2}] \qquad (5)$$

where gv and ga denote the vector and axial vector couplings of electrons or quarks,

$g = G_F / 8\sqrt{2}\,\pi\,\alpha = 4.49\cdot10^{-6}$ GeV^{-2} and

$\eta = (M_z^2 / s-M_z^2)$ is a propagator term sensitive to the mass of the Z^0.

Using the standard model and assuming $\sin^2\vartheta_w = 0.23$, the electroweak correction to R is about 1% to 2% at highest PETRA energies, but other values of $\sin^2\vartheta_w$ yield measureably large changes in R.

2.2. Search for 'open' top quark production

Since the total hadronic cross-section R is sensitive to the number of produced quark flavors, a measurement of this quantity is a good way to prove the existence of a new quark flavor. This is impressively demonstrated by Fig. 3, where the data at c.m. energies below $\sqrt{s} \approx 10$ GeV [15] show steps associated with the production of charm and bottom quarks. Narrow bound quark-antiquark states (ρ, ω, φ, J/Ψ, Ψ', Υ, Υ', Υ'') are also indicated in this figure as spikes.

In the PETRA and PEP energy range above $\sqrt{s}$ = 12 GeV all measurements [16-17] are consistent with R ≈ 3.9 (solid line) as expected from QCD for five different quark flavors. The production of top quarks would increase to R ≈ 5.3 (dashed line). The results of recent measurements [17-18] at highest PETRA energies from the different experiments are summarized in Table 1. The R-measurements indicate that until now we have not reached the open top continuum.

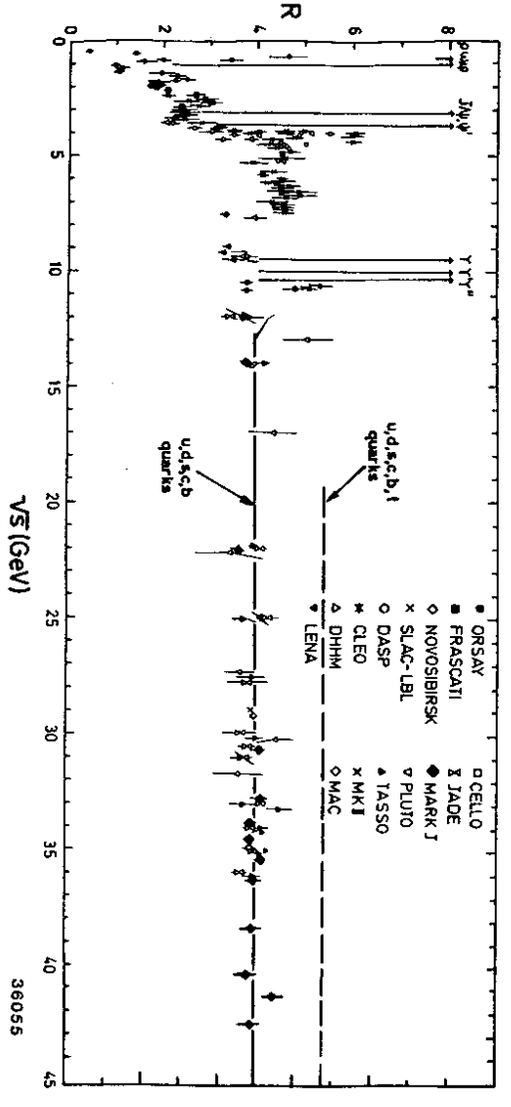

Figure 3: Total hadronic cross-section R as function of the c.m. energy $\sqrt{s}$.

Experiment	R-values 33.0 GeV - 36.7 GeV	37.9 GeV - 36.7 GeV
CELLO	3.85 ± 0.12	-------
JADE	3.99 ± 0.06	3.99 ± 0.21 *
MARK-J	3.91 ± 0.06	3.91 ± 0.19
TASSO	4.11 ± 0.06	4.00 ± 0.26 *
Average	3.99 ± 0.03	3.95 ± 0.13

Table 1: Hadronic cross-section R at highest PETRA energies. The stars indicate preliminary results. The errors quoted are statistical only. Normalisation errors are 2.5% to 6% for the various experiments.

The conclusion emerging from the R-measurements can be supported by the analysis of the spatial distribution of energy or momentum of hadronic final states. If massive open top quark pairs were produced we would expect not only an increase in R , but also an observable enhancement in the number of events with isotropic energy flow. Such a spatial energy distribution is expected if the virtual photon materializes into two very heavy quarks, each with a mass close to the beam energy. Such quarks would be produced almost at rest and their subsequent fragmentation leads to a spherical energy distribution. On the other hand, pairs of light quarks move at high speed and the Lorentz boost of their hadronic fragmentation products would result in narrow hadron jets collimated around the initial quark directions. A kinematic variable suited to describe the shape of hadronic events is thrust T [19] with the limits T = 0.5 for isotropic and T = 1.0 for collinear energy distribution.

The thrust distribution measured by the MARK-J collaboration at $\sqrt{s} \geq 39.79$ GeV is shown in Fig. 4 together with the predictions of QCD for five-flavor- and six-flavor-production. A quantitative comparison between the measurements and the expectations can be made using Table 2.

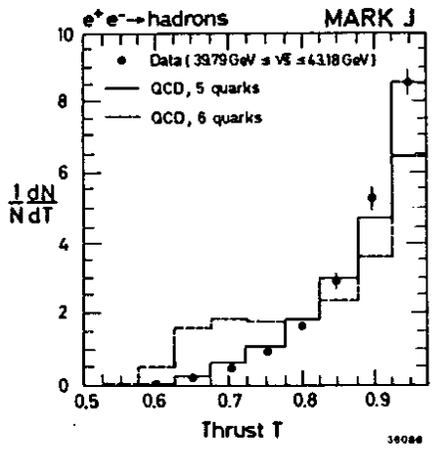

Figure 4: Thrust distribution of hadronic final states for $\sqrt{s} \geq 39.73$ GeV measured by MARK-J. The solid (dashed) histogram shows the expected distribution for five (six) quark flavor production in the framework of QCD.

Sample	Mean thrust	Number of events below T = 0.75
Data	0.899 ± 0.002	100
QCD, 5 quarks	0.897	113
QCD, 6 quarks	0.850	433

Table 2: Results of the thrust analysis of hadronic events. The analysis was performed by the MARK-J collaboration at c.m. energies between 39.79 GeV and 43.18 GeV. The expectations from QCD are based on $\sqrt{s}$ = 41 GeV and M_{Top} = 19 GeV.

Comparisons of the mean value of thrust and the number of events with $T \leq 0.75$ exclude the production of open top quarks below c.m. energies of around 40 GeV.

A similar analysis can be performed with the subsample of events containing muons, namely with inclusive muon hadron events:

$$e^+ e^- \longrightarrow \mu + \text{hadrons} \qquad (6)$$

The muons in these events originate from the semi-leptonic decay of heavy quarks: charm, bottom (and top). Fig. 5 sketches the decay of a bottom quark into an inclusive muon event.

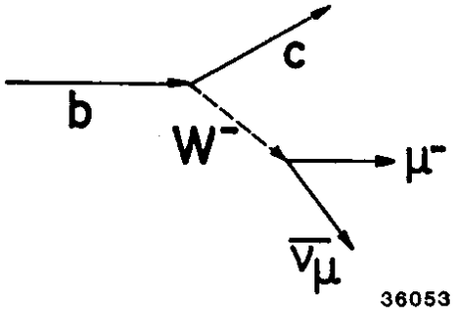

Figure 5: Semi-leptonic weak decay of bottom quark.

Thus also for these events the production of a new, heavy quark flavor would show up in a sudden increase of the production rate and a change of the event topology.

Fig. 6 shows the inclusive muon rate as function of the c.m. energy measured by the MARK-J group [20-21], together with expectations for five and six flavor production. Similar results have been obtained by the CELLO collaboration [22].

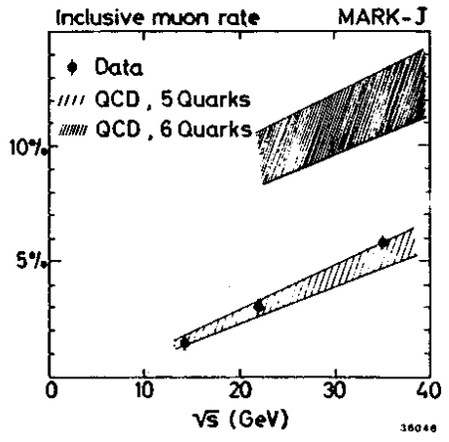

Figure 6: Inclusive muon rate as function of the c.m. energy $\sqrt{s}$. The data measured by the MARK-J group is compared to the expected rate for five and six quark flavor production.

The thrust distribution of inclusive muon events at c.m. energies between 37.94 GeV and 38.63 GeV [21] (Fig. 7) again shows good agreement with the five quark prediction and rules out the additional production of a top quark (see Table 3).

Sample	Mean thrust	Number of events below T = 0.75
Data	0.889 ± 0.012	1
QCD, 5 quarks	0.905	1.1
QCD, 6 quarks	0.800	13.4

Table 3: Results of the thrust analysis of inclusive muon events. The analysis was performed by MARK-J at c.m. energies between 37.94 GeV and 38.63 GeV. The expectations from QCD assume the mass of the top quark to be M_{Top} = 17 GeV.

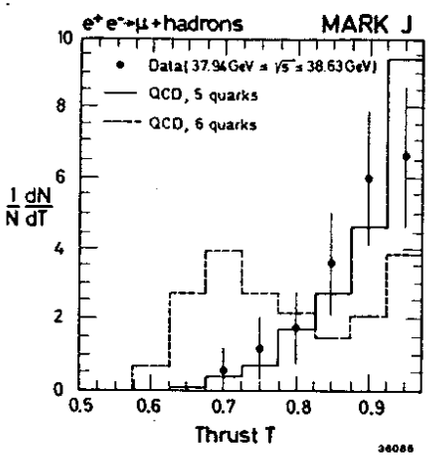

Figure 7: Thrust distribution of inclusive muon events. The data are compared to the predictions for five and six quark flavor production.

2.3. Models without top quarks

Until now all data presented do not show any evidence of the existence of top quarks. There are some models [23-24] in which the top quark does not exist and the bottom quark is put in a weak isospin singlet. In this case the bottom quark would decay weakly by a flavor-changing neutral current into another charge $-\frac{1}{3}$ e quark plus a fermion-antifermion pair. Fig. 8 sketches such a bottom decay with a muon pair in the finale state. The signature of such a decay would be a pair of oppositely charged muons imbedded in a hadron jet.

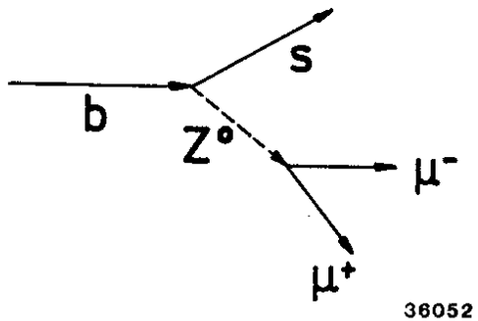

Figure 8: Flavor changing neutral current decay of a bottom quarks into a pair of muons.

Theoretical calculations [24] and measurements of the branching ratio of bottom quarks into single muons [20,25] lead to the prediction for the branching ratio of bottom quarks into μ-pairs: $B(b \longrightarrow \mu\mu X) \gtrsim 1\%$. Measurements performed by JADE[26] and MARK-J [27] give upper limits on this quantity (with 95% C.L.):

JADE: $B(b \longrightarrow \mu\mu X) \leq 0.7\%$.

MARK-J: $B(b \longrightarrow \mu\mu X) \leq 0.7\%$.

Thus no flavor-changing neutral decays of bottom quarks have been found. As a consequence of this conclusion five quark models in which the bottom quark is in a weak isospin singlet are ruled out, making it likely that the b quark is in a doublet with the top quark.

2.4. Search for 'hidden' top quarks

If current theories are accepted, the results discussed above lead to the conclusion that the top quark does exist, but that even the highest energies at PETRA are not sufficient to produce open top. Nevertheless it would be possible to find the top quark if it were to manifest itself as a set of narrow bound states of a top- and an antitop-quark ($t\bar{t}$) which thus carry a top quantum number equal to zero ('hidden' top). Interpretation of the vector mesons ρ, ω, φ, J/Ψ, Ψ', T, T' and T'' (see Fig. 3) as non-relativistic $q\bar{q}$ bound states leads to the prediction that the mass of the lowest bound state is a few GeV below the open top continuum [28]. These bound states can again be detected by measuring the hadronic cross-section, but, in contrast to continuum production,

this time they show up as spikes in R as the c.m. energy changes. The width of these narrow resonances is masked by the machine energy resolution.

In order to search for these narrow resonances four energy scans were performed in steps of 20 MeV (below $\sqrt{s}$ = 37 GeV) and 30 MeV (above $\sqrt{s}$ = 37 GeV) in c.m. energy in the ranges:

$$29.90 \text{ GeV} \leq \sqrt{s} \leq 31.46 \text{ GeV}$$
$$33.00 \text{ GeV} \leq \sqrt{s} \leq 36.72 \text{ GeV}$$
$$37.94 \text{ GeV} \leq \sqrt{s} \leq 38.63 \text{ GeV}$$
$$39.79 \text{ GeV} \leq \sqrt{s} \leq 43.18 \text{ GeV}$$

The results of the first two scans have been reported already [16-17].

The R-measurements around 38 GeV are shown in Fig. 9 and first preliminary results above 39.79 GeV are displayed in Fig. 10. Upper limits on the production cross-section were obtained by fitting the function

$$R = R_0 + R_{Res}(\Gamma_{ee} \cdot B_h) \qquad (7)$$

where R_0 represents the constant continuum production and $R_{Res}(\Gamma_{ee} \cdot B_h)$ is the function describing the expected toponium resonance after including corrections for the machine energy spread and radiative effects [29]. Γ_{ee} is the decay width into $e^+ e^-$ and B_h is the hadronic branching ratio.

Combining the R-measurements of JADE, MARK-J and TASSO we find that in the third energy scan the most prominent 'resonance signal' is at a c.m. energy $M_{Res.}$ = 38.36 GeV and results in an upper limit of $\Gamma_{ee} \cdot B_h \leq 0.8$ keV (90% C.L).

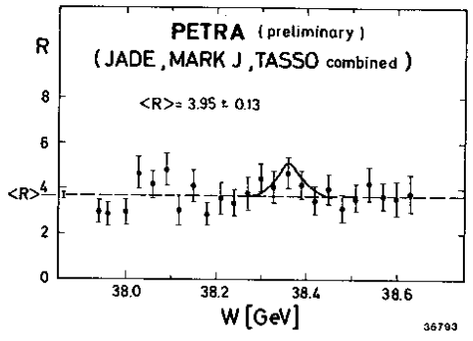

Figure 9: Combined hadronic cross-section R measured in an energy scan between 37.94 GeV and 38.63 GeV. The dashed line indicates the mean value, the solid line represents the most prominent 'resonance signal'.

The fits of the R-measurements above 39.79 GeV using only the data obtained by the MARK-J group give $M_{Res.}$ = 41.184 GeV and $\Gamma_{ee} \cdot B_h \leq 2.7$ keV (95% C.L).

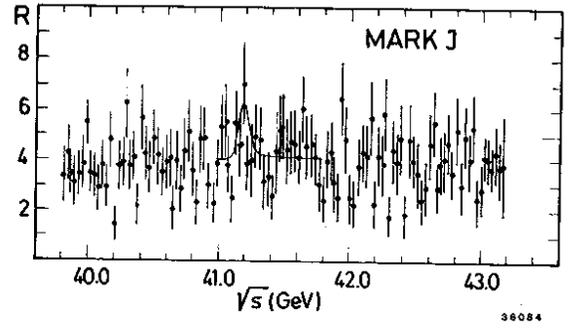

Figure 10: R-measurements obtained by MARK-J in the energy scan above 39.79 GeV. The solid curve indicates the results of the fit.

On the basis of the experimental fact that Γ_{ee}/Q_l^2 is approximately 10 keV for the vector meson ground states ρ, ω, φ, J/Ψ and T (which also can be described by models [28]), and based on the expectation that B_h is of order 80% [30], the production of a ground state ($t\bar{t}$) resonance should give $\Gamma_{ee} \cdot B_h \approx 3.5$ keV and is therefore excluded by the data shown in Figs. 9 and 10.

2.5. Electroweak effects

The total hadronic cross-section is not only a sensitive quantity for detecting new quark flavors, but can also be used to study electroweak effects. The production cross-section of a quark of flavor i depends also on the vector and axial vector couplings of electrons and quarks (eq. 5). In the framework of the Glashow-Weinberg-Salam model the couplings can be expressed in terms of the electroweak mixing angle $\sin^2\vartheta_w$ (Table 4).

Particle	gv	ga
electron	$-1/2 + 2 \cdot \sin^2\vartheta_w$	$-1/2$
u c (t) quark	$1/2 - 4/3 \cdot \sin^2\vartheta_w$	$1/2$
d s b quark	$-1/2 + 2/3 \cdot \sin^2\vartheta_w$	$-1/2$

Table 4: Vector and axial vextor couplings of the electron and quarks.

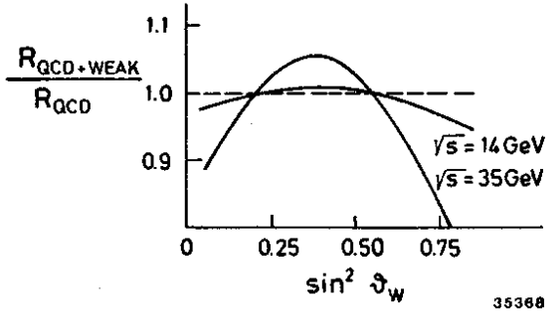

Figure 11: Dependence of the hadronic cross-section on $\sin^2\vartheta_w$ for two different c.m. energies.

Figure 11 shows the variation of R with $\sin^2\vartheta_w$ for two different c.m. energies. Although even at highest energies the effect seems to be too small to be observed, the hadronic cross-section increases by 11%, if $\sin^2\vartheta_w$ changes from 0.10 to 0.30. Taking systematic errors on the R-measurements of about 2.5% to 6% into consideration, this increase is still rather small. However, the main source of the systematic error, the uncertainty in the normalisation, is independent of the c.m. energy, whereas the contributions of the weak interaction to R increase with the square of the c.m. energy. Thus the energy dependence of R allows a measurement of $\sin^2\vartheta_w$.

Using eq. 5 and summing over all quark flavors and colors, the fits to the R measurements give the values of $\sin^2\vartheta_w$ as listed in Table 5 [31].

Experiment	$\sin^2\vartheta_w$	α_s
JADE	0.23 ± 0.05	0.20 ± 0.08
MARK-J	$0.28 + 0.08 - 0.05$	0.13
TASSO	$0.40 \pm 0.15 \pm 0.02$	0.17

Table 5: Fits of $\sin^2\vartheta_w$ using the hadronic cross-section R. The JADE result is obtained by a simultaneous fit of $\sin^2\vartheta_w$ and α_s. The fits of $\sin^2\vartheta_w$ performed by MARK-J and TASSO use a fixed value of α_s at $Q^2 \approx 1000$ GeV^2.

Fig. 12 shows the measured R-values at PETRA and compares with the predictions of QCD including contributions from the weak interaction using different values of $\sin^2\vartheta_w$.

This figure also shows clearly the need to perform measurements at higher energies where advantage can be taken of the higher sensitivity to electroweak effects which result in a more precise determination of $\sin^2\vartheta_w$.

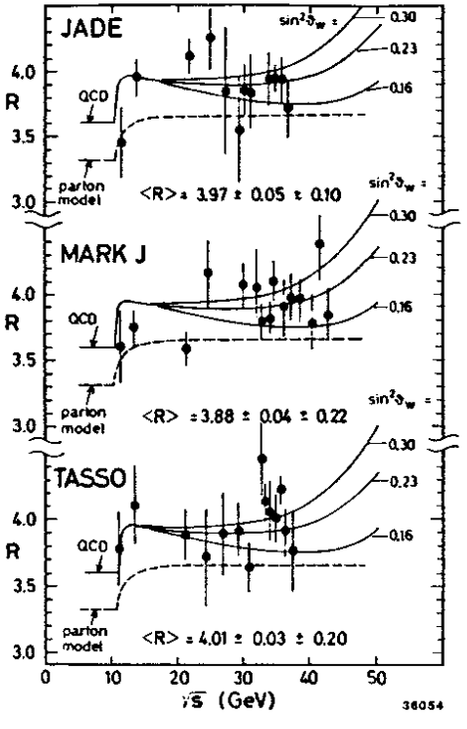

Figure 12: Hadronic cross-section R measured by JADE, MARK-J and TASSO compared to the predictions of the quark parton model (dashed line) and the QCD predictions (using α_s = 0.17), where the contribution from the weak interactions is included using different values of $\sin^2\vartheta_w$.

Although the precision of the PETRA measurements of $\sin^2\vartheta_w$ are not competetive with the results of neutrino-nucleon or electron-deuteron or $\bar{p}$-p experiments, the measurements do support the validity of the standard model and its applicability in the high Q^2-region up to 1200 GeV^2. Furthermore the PETRA experiments also measure the couplings of the heavy quarks which contribute about 45% to the total hadron event sample.

3. TWO PHOTON INTERACTIONS

3.1. Resonance production

The basic diagram of the two photon interactions at $e^+ e^-$ colliding beams is shown in Fig. 13. Both, the incoming electron and positron radiate a photon predominantly at small angles with respect to the beam axis and with small energies. The radiated photons interact and produce a final state X.

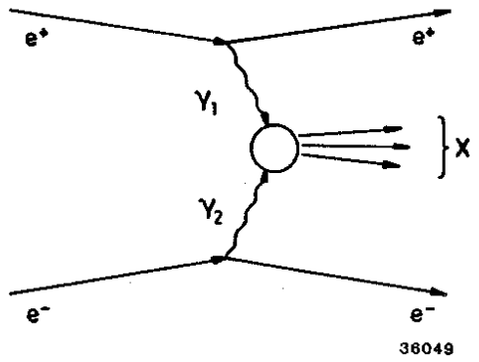

Figure 13: Basic diagram for two photon interactions producing a final state X.

Here only resonant meson production will be discussed. Because of the well defined initial state the resonance quantum numbers are restricted to:

$$J^{PC} = 0^{-+},\ 0^{++},\ 2^{-+},\ 2^{++},\ \ldots \qquad (8)$$

I shall present recent results on two members of the 2^{++} meson nonet, the f and A_2. Results on other resonances have been reported at various conferences [32-33].

The JADE collaboration detects a clear f signal over a very small background by studying the decay:

$$f \longrightarrow \pi^0\,\pi^0 \longrightarrow \gamma\gamma\,\gamma\gamma \qquad (9)$$

The events were selected [34] from the data sample by demanding four photons each with an energy greater than 100 MeV in the angular range of $|\cos\vartheta| \leq 0.76$. Fig. 14a shows the mass spectrum

of all $\gamma\gamma$ combinations (six per event). Only those events with two opposite $\gamma\gamma$ combinations, each lying in the π^0 band between 0.09 GeV/c^2 and 0.19 GeV/c^2, are shown in Fig. 14b. This figure clearly exhibits a resonance signal in the invariant $\pi^0\pi^0$ mass-spectrum, which is associated with resonant f production. Other PETRA groups [35] detect the f meson by searching for its decay into two oppositely charged pions and obtain compatible results.

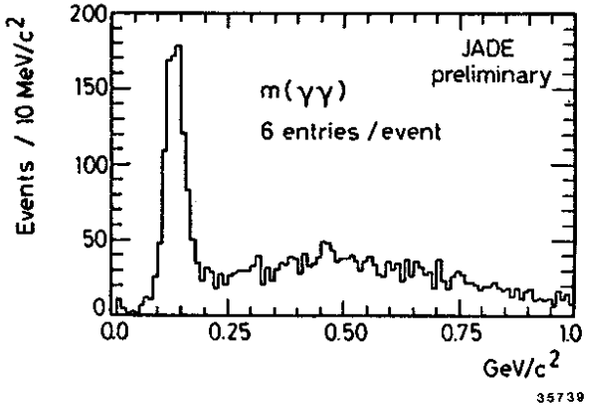

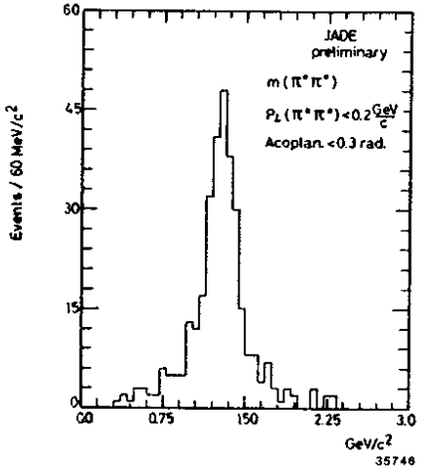

Figure 14: Invariant mass spectra measured by the JADE group for four-photon final states:

a) m($\gamma\gamma$) with a clear π^0 peak.

b) m($\pi^0\pi^0$) showing a pronounced f signal.

Another neutral meson of the 2^{++} nonet, the A_2, is seen by the JADE collaboration which studies the decay chain:

$$A_2 \longrightarrow \rho^{\pm}\,\pi^{\mp} \longrightarrow \pi^+\,\pi^-\,\pi^0 \qquad \longrightarrow \gamma\gamma \qquad (10)$$

Fig. 15 demonstrates the basic principles of the analysis. First, the mass spectrum of the $\gamma\gamma$-system is determined. Then those events lying within the indicated π^0-band of Fig. 15a are used to calculate the $\pi^{\pm}\pi^0$ mass. This mass spectrum, shown in Fig. 15b (two combinations per event), has a clear $\rho^{\pm}$ peak. The resultant mass measurements of the 3π system, Fig. 15c, finally exhibit the A_2 peak. The open histogram includes all events used in Fig. 15b, whereas the shaded histogram represents only those events with at least one $\pi^{\pm}\pi^0$ combination within the $\rho^{\pm}$ band between 0.55 GeV/c^2 and 0.95 GeV/c^2. Similar results have been obtained by the CELLO collaboration [36].

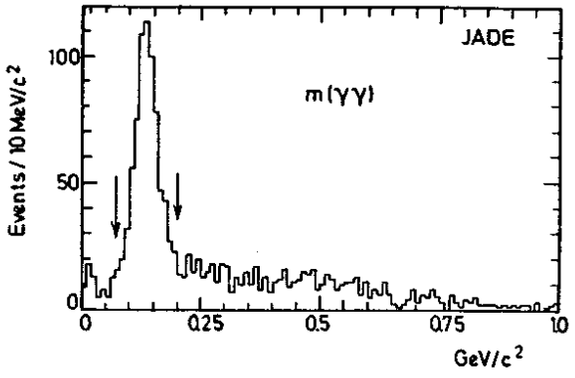

Figure 15: Invariant mass spectra measured by JADE in studying the reaction $e^+e^- \longrightarrow e^+e^-\pi^+\pi^-\gamma\gamma$

a) $m(\gamma\gamma)$. The π^0 mass band is indicated by arrows.

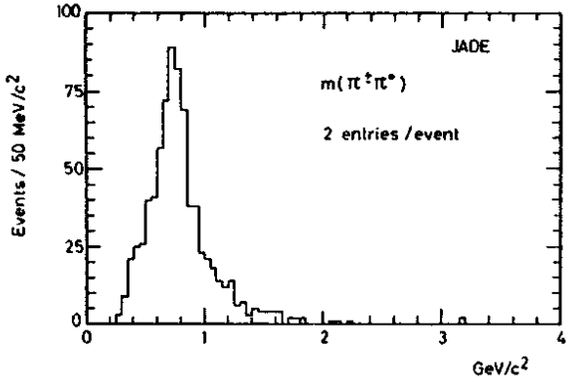

b) $m(\pi^\pm\pi^0)$ showing a clear $\rho^\pm$ peak.

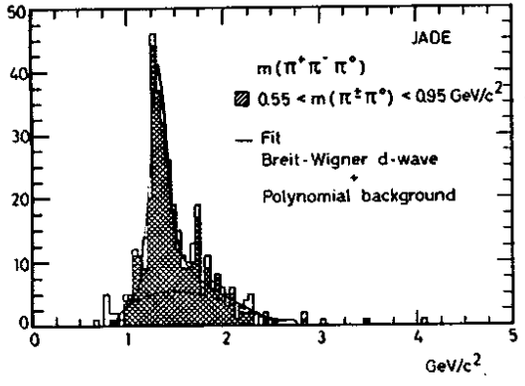

c) $m(\pi^+\pi^-\pi^0)$. The open histogram represents all events from Fig. 15b, whereas the hatched histogram shows the invariant mass of those events lying in the $\rho^\pm$ band.

One of the prime objectives for analysing resonances R in two-photon interactions is to measure the radiative width $\Gamma_{R\gamma\gamma}$. Recent results [33,35-38] for the f and A_2 meson are listed in Table 6.

Experiment	Radiative decay widths (in keV) f resonance	A_2 resonance
CELLO	2.7 ± 0.2 ± 0.2 *	0.81 ± 0.19 ± 0.27
JADE	2.3 ± 0.2 ± 0.5 *	0.84 ± 0.07 ± 0.15 *
PLUTO	2.3 ± 0.5 ± 0.35	----------
TASSO	3.2 ± 0.2 ± 0.6	----------
Average	2.64 ± 0.22	0.83 ± 0.14

Table 6: Radiative decay widths measured at PETRA. The stars indicate preliminary results. The errors quoted by the experiments are devided into statistical and systematic errors. The averages take both errors into account.

An interesting quantity is the ratio of the average radiative widths measured as

$$\frac{<\Gamma_{A2\gamma\gamma}>}{<\Gamma_{f\gamma\gamma}>} = 0.31 \pm 0.06 \qquad (11)$$

This value can be compared with the expectation from SU(3) with ideal mixing including phase space corrections namely:

$$\frac{\Gamma_{A2\gamma\gamma}}{\Gamma_{f\gamma\gamma}} = 0.40 \qquad (12)$$

Thus, by measuring the ratio of the decay widths precisely, it is possible to determine the mixing angle of the 2^{++} nonet.

3.2. The photon structure function

Measurements of deep inelastic electron photon scattering

$$e + \gamma \longrightarrow e + \text{hadrons} \qquad (13)$$

may be used to test the predictions of QCD [37]. The cross-section for this process at high Q^2 can be calculated by perturbative QCD[38] since it is dominated by the pointlike contribution.

Reaction (13) can be described approximately in terms of the two-photon initiated hadron production, which is sketched in Fig. 16. One of the incoming particles radiates a hard photon (γ_1) and is therefore scattered away from the initial direction by an angle ϑ and its energy is reduced from E_b to E'. The other incoming particle radiates a soft photon (γ_2) and remains undetected inside the beam pipe. Both the photons interact and produce a hadronic system having an energy W. These events can be isolated by searching for 'single tag' hadron events, i.e. hadronic final states with an additional electron at small scattering angles.

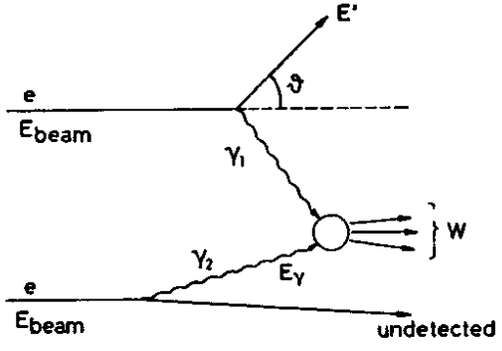

Figure 16: Feynman diagram of single tag hadronic final states used to approximate the deep inelastic electron photon reaction.

The kinematics of these events is described by the quantities:

$$Q^2 = 4 \cdot E_b \cdot E' \cdot \sin^2 \vartheta/2$$

$$x = \frac{Q^2}{Q^2 + W^2}$$

$$y = 1 - \frac{E'}{E_b} \cdot \cos^2 \vartheta/2 \qquad (14)$$

and the double differential cross-section can be expressed in terms of structure functions [39]:

$$\frac{d\sigma}{dx \cdot dy} = \frac{16 \cdot \pi \cdot \alpha^2}{Q^4} E_b \cdot E_\gamma \left[(1 - y) \cdot F_2 + x \cdot y^2 F_1 \right] \qquad (15)$$

Since the electron is tagged at small scattering angles ϑ, where y^2 is less than 0.10, the results that will be shown neglect the F_1 term.

Comparisons between the data and various theoretical predictions are usually made by determining the x_{vis} distribution defined as:

$$x_{vis} = \frac{Q^2}{Q^2 + W_{vis}^2} \qquad (16)$$

where W_{vis} denotes the measured energy of the hadronic system. Q^2 is the momentum transfer squared calculated from the energy E' and the polar angle ϑ of the scattered electron.

Fig. 17 shows the x_{vis} distribution at an average Q^2 of 24 GeV^2 measured by the JADE collaboration [39] together with the expectations from the quark parton model (QPM), leading order (LOQCD) and higher order QCD (HOQCD), both for Λ-values of 0.28 GeV. This figure also shows the predictions using a 'mixed model' which describes the light quarks (u, d and s) in the framework of QCD and adds the c quark contribution from the quark parton model.

All the curves agree quite well except for the lowest x_{vis}-bin which might be effected by the hadronic component of the photon. Since the Monte Carlo curves are sensitive to the QCD scale parameter Λ it can in principle be determined from this analysis. On the other hand this data does not show the necessity to describe the distribution by the QCD predictions since the QPM model fits similarly well.

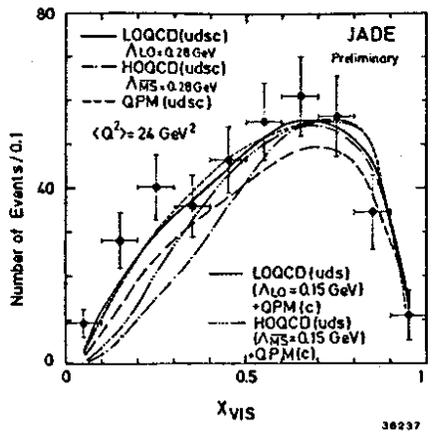

Figure 17: The x_{vis} distribution measured by JADE compared with the expectations from the quark parton model (QPM), leading order QCD (LOQCD), higher order QCD (HOQCD) and the 'mixed model'.

Recent measurements performed by JADE[39] at an average Q^2 of 100 GeV^2 are shown in Fig. 18. Also for these measurements the QPM-curve is in agreement with the data. The LOQCD predictions are drawn as a band limited by the curves of two extreme Λ-values (0.02 GeV and 0.20 GeV) and describe the data quite well. Similarly as the data at lower Q^2 there is no preference to use a particular model to describe the measurements.

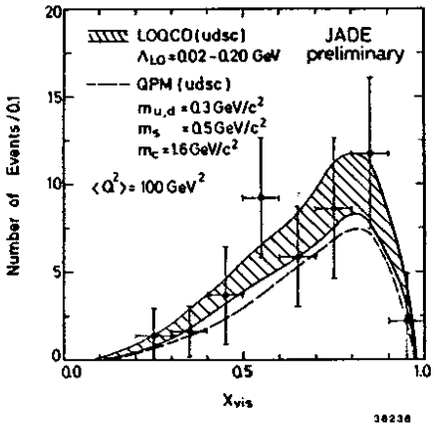

Figure 18: The measured x_{vis} distribution and predictions from leading order QCD (LOQCD) for Λ-values between 0.02 GeV and 0.20 GeV. The dashed curve represents the expected distribution using the quark parton model (QPM).

Unfortunately the theoretical predictions do have some shortcomings. The most critical seems to be the neglect of quark mass effects in the description of the photon structure function $F_2(x,Q^2)$ in both, the leading order [40] and the higher order QCD [41] calculations. This treatment is an approximation

certainly not justified for the c quark. In order to take its mass effects into consideration analyses have been carried out by CELLO[42], JADE[39], PLUTO [43] and TASSO [44] using a 'mixed model', which combines the LOQCD distribution for the light quarks (u, d and s) and a quark parton model description for the c quark. It has been found that the mixed model describes the measurements quite well, but the data does not favor it against LOQCD.

The various theoretical descriptions give rise to a range of Λ-values between 0.07 GeV and 0.28 GeV [39,42]. Restricting attention to the mixed model we get:

CELLO: $\Lambda = (0.13 + 0.07 - 0.05)$ GeV

JADE: $\Lambda = (0.15 + 0.07 - 0.05)$ GeV

Finally the $\ln Q^2$-dependence of $F_2(Q^2)$ predicted by LOQCD as well as the QPM can be tested by averaging the photon structure function over a certain x_{vis}-range. The results of the measurements performed at PETRA [45] are shown in Fig. 19 and are compatible with the expected logarithmic variation, without demonstrating the existence of such a dependence.

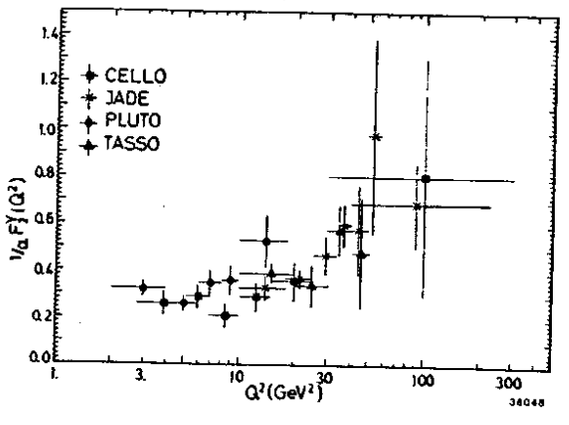

Figure 19: The photon structure function F_2 as a function of Q^2 measured at PETRA.

4. CONCLUSIONS

The results of the PETRA experiments discussed may be summarized as follows:

No open top quark production up to $\sqrt{s} \approx 40$ GeV.

However, the top quark must exist in an isospin doublet together with the bottom quark.

The top-antitop ground state has not been detected in the energy regions scanned.

The hadronic cross-section R also measures the couplings of heavy quarks and the $\sin^2\vartheta_w$ values are in agreement with other experiments.

Clear signals of the f and A_2 resonances are seen. The ratio of their radiative widths is as expected from SU(3) with ideal mixing.

Analyses of deep inelastic electron photon scattering give Λ-values compatible with those obtained in deep inelastic lepton nucleon scattering experiments.

The measured photon structure function $F_2(Q^2)$ does indicate the expected logarithmic Q^2 dependence.

Acknowledgements

I would like to thank the members of the CELLO, JADE, PLUTO and TASSO collaborations as well as my colleagues from the MARK-J experiment for providing me their (partially unpublished) data. I am very grateful to Drs. G.Grindhammer, H. Kolanoski, P.Mättig, M.Minowa, T.Nozaki, J.Olsson and W.Wagner for their valuable support preparing this review. I wish to thank Dr. D.P.Barber, M.Capell and Prof. M.Chen for their critical reading of the manuscript. I also thank the directors of DESY, Prof. V.Soergel and Prof. P.Söding, for their hospitality. Finally I wish to thank Prof. K.K.Phua for an enjoyable and inspiring conference at Singapore.

References

1. S.D.Drell, D.J.Levy and T.M.Yan, Phys.Rev.137, 2159(1969) and Phys.Rev.D1, 1617(1970).
2. N.Cabibbo, G.Parisi and M.Testa, Lett.Nuovo Cimento 4, 35(1970).
3. J.D.Bjorken and S.J.Brodsky, Phys.Rev.D1, 1416(1970).
4. R.P.Feynman, Photon-Hadron Interactions, Benjamin, Reading Mass., 1972.
5. J.Ellis, M.K.Gaillard and G.G.Ross, Nucl.Phys.B111, 253(1976) and erratum B130, 516(1977).
6. T.A.DeGrand, Yee Jack Ng and S.H.H.Tye, Phys.Rev.D16, 3251(1977).
7. J.Kogut and L. Susskind, Phys.Rev.D9, 697, 3391(1974).
8. A.M.Polyakov, Proceedings of the 1975 International Symposium on Lepton and Photon Interactions at High Energies, Stanford, August 1975.
9. K.G.Chetyrkin et al., Phys.Lett.85B, 277(1979).
10. M.Dine and J.Sapierstein, Phys.Lett.42, 668(1979).
11. W.Celmaster and R.Gonsalves, Phys.Lett.44, 560(1980).
12. W.Bartel et al., Phys.Lett.119B, 239(1982) – B.Adeva et al., Phys.Rev.Lett.50, 2051(1983) – M.Chen, talk at this conference.
13. R.Budny, Phys.Lett.55B, 227(1975).
14. J.Ellis and M.K.Gaillard, "Physics with Very High Energy e^+e^- Colliding Beams", CERN 76-18(21).
15. A.Quenzer, thesis, Orsay Report LAL, 1299(1977) – A.Cordier et al., Phys.Lett.81B, 389(1979) – V.A.Sidorov, Proceedings of the XVIII International Conference on High Energy Physics, Tiblisi, USSR, B13 (1976) – R.F.Schwitters, Proceedings of the XVIII International Conference on High Energy Physics, Tiblisi, USSR, July 1976 – J.Perez-Y-Jorba, Proceedings of the XIX International Conference on High Energy Physics, Tokyo, 1978 – J.Burmester et al., Phys.Lett.66B, 395(1977) – R.Brandelik et al., Phys.Lett.76B, 361(1978) – J.Siegrist, Report No. SLAC-225(1979) – H.Albrecht et al., DESY-Report 82-037(1982).

16. Ch.Berger et al., Phys.Lett.86B, 413(1979) and Phys.Lett.91B, 148(1980) – J.D.Burger, Proceedings of the XXI International Conference on High Energy Physics, Paris, 1982, C3-63 – G.Heinzelmann, Proceedings of the XXI International Conference on High Energy Physics, Paris, 1982, C3-59 – D.M.Ritson, Proceedings of the XXI International Conference on High Energy Physics, Paris, 1982, C3-52 – G.H.Trilling, Proceedings of the XXI International Conference on High Energy Physics, Paris, 1982, C3-57 – For details of analysis see for example: H.Rykaczewski, Paricles and Fields 2, Plenum Press, 621 (1983) and references therein.
17. R.Brandelik et al., Phys.Lett.113B, 499(1982) – H.J.Behrend et al., DESY-Report 81-029(1981).
18. B.Adeva et al., Phys.Rev.Lett.50, 799(1983) – W.Bartel, private communication – W.Bartel et al., DESY-Report 83-050(1983).
19. E.Farhi, Phys.Lett.39, 1587(1977) – S.Brandt et al., Phys.Lett.12, 57(1964) – S.Brandt and H.Dahmen, Zeitschr. f. Physik C1, 61(1979).
20. B.Adeva et al., Phys.Rev.Lett.51, 443(1983).
21. J.Salicio, private communication
22. H.J.Behrend et al., DESY-Report 83-034(1983).
23. V.Barger et al., Phys.Rev.D24, 1328(1981) – H.Georgi and S.Glashow, Nucl.Phys.B167, 173(1980) – H.Georgi and A.Pais, Phys.Rev.D19, 2746(1979) – J.D.Bjorken and K.Lane, Proceedings of the International Neutrino Conference, Baksan, 1977 – F.Gürsey et al., Phys.Lett.60B, 177(1970).
24. G.L.Kane and M.E.Peskin, Nucl.Phys.B195, 29(1982).
25. K.Chadwick et al., Phys.Rev.D27, 475(1983) – D.Lüke, Proceedings of the XXI International Conference on High Energy Physics, Paris, 1982, C3-67
26. W.Bartel et al., DESY-Report 83-049(1983).
27. B.Adeva et al., Phys.Rev.Lett.50, 799(1983).
28. D.R.Yennie et al., Phys.Rev.Lett.34, 239(1975) – F.E.Close et al., Phys.Lett.62B, 213(1976) – M.Kramer et al., DESY-Report 80-25(1980) – W.Buchmüller and S.-H.H.Tye, Fermilab-Pub-80/94-THY(1980).
29. J.D.Jackson and D.L.Scharre, Nucl.Instrum.Methods B128, 13(1975).
30. J.P.Leveille, University of Michigan Report No. UM-HE-81-11 (to be published).

31. R.Brandelik et al., Phys.Lett.113B, 499(1982) – W.Bartel et al., DESY-Report 83-050(1983).
32. D.J.Burke, Proceedings of the 4th International Colloquium on $\gamma\gamma$ Interactions, Paris, 1981, 123 – E.Hilger, Proceedings of the 4th International Colloquium on $\gamma\gamma$ Interactions, Paris, 1981, 149 – R.J.Wedemeyer, Proceedings of the International Conference on Lepton and Photon Interactions at High Energies, Bonn, 1981, 410 – J.Olsson, Proceedings of XVIIth Rencontre de Moriond (Les Arcs, Savoie), 13(1982).
33. J.Olsson, DESY-Report 83-076(1983) and Proceedings of the 5th International Workshop on Photon-Photon Collisions, Aachen, 1983 (to be published).
34. T.Nozaki, DESY-Report 83-011(1983).
35. Ch.Berger et al., Phys.Lett.94B, 254(1980) – R.Brandelik et al., Zeitschr. f. Physik C10, 117(1981). – F.Kovacs, Proceedings of the 5th International Workshop on Photon-Photon Collisions, Aachen, 1983 (to be published).
36. H.J.Behrend et al., Phys.Lett.114B, 378(1982) and erratum Phys.Lett.125B, 518(1983).
37. A.J.Buras, Proceedings of the International Conference on Lepton and Photon Interactions at High Energies, Bonn, 1981 – W.R.Frazer, Proceedings of the 4th International Colloquium on $\gamma\gamma$ Interactions, Paris, 1981.
38. C.Petersen et al., Nucl.Phys.B174, 424(1980).
39. W.Bartel et al., Phys.Lett.121B, 203(1983) – JADE Collaboration, private communication.
40. E.Witten, Nucl.Phys.B120, 189(1977). – C.H.Llewellyn Smith, Phys.Lett.79B, 83(1978) – W.R.Frazer and J.Gunion, Phys.Rev.D20, 147(1979) – R.J.Dewitt et al., Phys.Rev.D19, 2046(1979).
41. W.A.Bardeen and A.J.Buras, Phys.Rev.D20, 166(1979) – D.W.Duke and J.F.Owens, Phys.Rev.D22, 2280(1980) – T.Uematsu and T.F.Walsh, Fermilab-Pub-81/55-THY(1981).
42. H.J.Behrend et al., Phys.Lett.118B, 211(1982) – H.J.Behrend et al., DESY-Report 83-018(1983).
43. W.Wagner, private communication – Ch.Berger et al., Phys.Lett.107B, 168(1981).
44. H.Kolanoski, private communication.
45. W.Wagner, Proceedings of the 5th International Workshop on Photon-Photon Collisions, Aachen, 1983 (to be published).